Full Paper

Propellants, Explosives, Pyrotechnics

DOI: 10.1002/prep.201900050

Characterization of Interfacial Micro-Structures of Explosive-Binder Composites by Gas Permeation

Shichun Li,[a] Jinjiang Xu,[a] and Yu Liu*[a]

Abstract: The interface between explosive and binder in plastic-bonded explosives (PBXs) plays an important role in their properties such as thermal and mechanical stability, and also their performance in detonation processes. However, characterization of their interfacial micro-structures remains challenging, due to the sensitive nature of the explosive material, and the extremely thin nature of the interface. This work demonstrates a concept of characterizing interfacial structures between explosives and binders by gas permeation. The N_2 permeability data of composite films of cyclotetramethylene-tetranitramine (HMX) particles dispersed in fluororubber binder (copolymers of vinylidene fluoride and chlorotrifluoro-ethylene, F2311) were tested and fitted by using gas transport mechanism theory, e.g. the Hashemifard-Ismail-Matsuura (HIM) model, and the Knudsen diffusion equation. The results indicate the presence of voids of thickness 2.2 nm between HMX and F2311, consistent with the results of neutron reflection and thermal conductivity measurements. These interfacial voids are considered to be related to the surface roughness of HMX particles. This work provides an alternative characterization technique for, as well as a new insight into, the interface between HMX and F2311.

Keywords: Plastic-bonded explosive · HMX · Interfacial voids · Characterization · Gas permeation

1 Introduction

Plastic-bonded explosives (PBXs), a type of polymer-matrix composite, consist of explosive particles dispersed in continuous polymer binder. The interfacial structures present within PBXs play a significantly important role in their properties and performance [1–3]. This is because of the inherently large particle surface area to volume ratio of PBXs, due to high loadings (>80% by weight) with micron-size explosive particles [4]. Cracks, an serious issue in PBX materials, tend to propagate along the interfaces and eventually lead to the failure of the material, which has been confirmed by both experimental observation and theoretical simulation [1,5–8]. Besides reducing mechanical stability, differences in interfacial structure may also cause different thermal and detonative processes, such as phase transformation of explosive crystals [2], deflagration propagation [9], and hot spot formation [10]. Thus, the interface of PBXs continuously attracts the attention of researchers in the field of energetic materials.

Considerable efforts have been made to characterize the interface between explosives and polymer binders. The intrinsic interfacial interaction, expressed by adhesion work, and the adhesive Hamaker constant, have been studied in particular. The thermodynamic adhesion work of binders with explosives, defined as the increase in free energy of the system caused by the creation of two new surfaces, is usually estimated by contact angle measurements [11,12]. The adhesive Hamaker constant, which determines the magnitude of the van der Waals interactions between components, is usually measured by Lifshitz theory, inverse gas chromatography, and contact angle measurements [13].

Besides intrinsic interfacial interactions, the surface structures of the explosive component, e.g. the roughness, also plays an important role in determining the interfacial structures formed within PBXs, as does material processing techniques [6]. These interfacial structures have been studied in multiple scales, from nanometre to centimetre, by utilizing several characterization techniques [5,14–17]. Positron annihilation lifetime spectroscopy (PALS), neutron scattering, x-ray computed tomography, and microscopy, have all been employed, though the sensitive nature of explosives and the thin, i.e. nanoscale, nature of the interface means thorough characterization remains challenging.

Neutron reflectometry (NR) has proven useful in the identification of interfacial structures between explosives and binders [2,4,6,18], as it is able to probe nanoscale structure. An intermixing phase (~60 Å) between cyclotetramethylene-tetranitramine (HMX) and poly(ester urethane) (Estane 5703) was observed by NR, which is attributed to the dissolution of HMX in the solution of Estane during sample preparation [18]. However, the application of NR is restricted by the limited penetration distance of neutrons, i.e. ~500 nm, and only thin explosive films can be

[a] *S. Li, J. Xu, Y. Liu*
Institute of Chemical Materials
China Academy of Engineering Physics
Mianyang 621900, P. R.China
**e-mail: liuyu307@caep.cn*

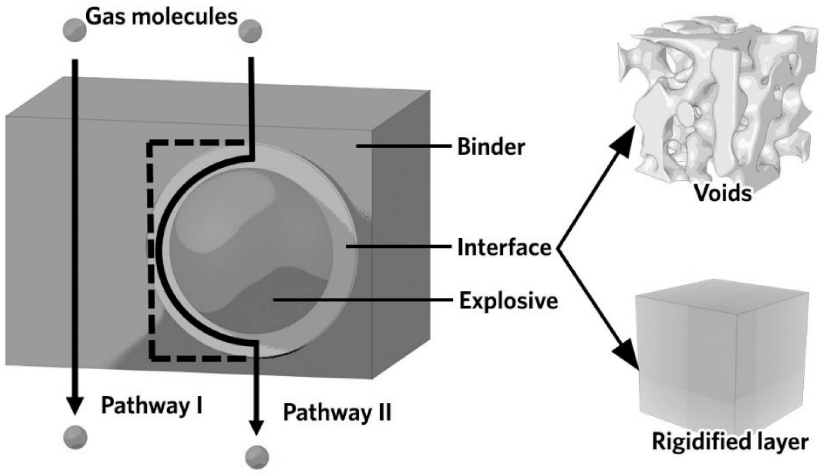

Figure 1. Schematic diagram of gas transport pathways in the explosive and binder composites, and non-ideal interfacial morphologies. In pathway II, gas molecules prefer transport along the solid line, i.e. interfacial voids, while the dash line indicates contact with a rigidified layer.

used for NR tests in place of bulk crystals [16]. Thus, an alternative technique suitable for characterization of the interfacial structures present in PBX materials is highly sought after.

Here, we propose a new concept of characterizing the interfacial structures between explosive and binder, by gas permeation. In the research field of membranes for gas separation, the fundamentals of gas transport in polymer based composites, i.e. polymer films containing dispersed particles, also known as mixed matrix membranes (MMMs), have been intensively studied [19]. A number of reliable models that descript the relationship between gas permeation rate, known as gas permeability or gas permeance, and structures have been established, and the models perform well in predicting the gas permeability of MMMs, in many cases [19–22]. As PBXs and MMMs possess essentially the same composite structure, i.e. particles dispersed in continuous polymer phase, these gas transport models are expected to be applicable in characterizing PBXs.

The gas permeation technique has been explored to characterize the pores and cracks in PBXs undergoing thermal damage [23–25]. In these works [23–25], the gas permeability of PBXs was tested with simultaneous heating that results in thermal damage to PBXs, and Darcy's law was used to relate the gas permeability with macroscale defects. However, different from previous works that focus on mesoscale and macroscale voids in PBXs, this work aims to characterize the nanoscale interface between explosives and binders. As shown in Figure 1, there are two pathways for gas molecules going through the 'defect-free' composite of explosive and binder: (i) the bulk phase of binder, and (ii) the interface between the explosive and the binder. As the diameter of gas molecule is less than 1 nm, e.g. kinetic diameter of 3.64 Å for N_2, interfacial voids, or the rigidified layer displayed in Figure 1, would strongly affect the transport of gas molecules that go through these interfacial structures [19].

Specifically, interfacial voids occuring due to poor adhesion of binder with explosive, would accelerate the transport of gas molecules through the solid line of pathway II, while a rigidified layer that presents due to strong adhesion of binder with explosive would retard the transport of gas molecules through the dash line of pathway II. Thus, by analysing the gas permeability of the composite through gas transport models, both the type of non-ideal interfacial structures, i.e. voids or a rigidified layer, and the thickness of this interfacial layer, can be obtained [19].

In order to demonstrate our concept, the gas permeability of a fluororubber (copolymers of vinylidene fluoride and chlorotrifluoro-ethylene with molar ratio of 1:1, F2311) film and a series of HMX-F2311 composite films containing different volume fraction of HMX was tested by using pure N_2. The gas permeability was fitted by using Hashemifard-Ismail-Matsuura (HIM) model and Knudsen diffusion equation [19]. The fitting result suggests that a voids containing interface layer with thickness of 2.2 nm presents in the HMX-F2311 composites, and the results have been discussed by associating with NR and atomic force microscope (AFM) results reported in the literatures [18, 26].

2 Experimental Section

2.1 Materials

HMX with average particle diameter of 1.36 μm and density of 1.90 g/cm^3, and F2311 with density of 2.03 g/cm^3 were provided by the Institute of Chemical Materials, China Academy of Engineering Physics. Ethyl acetate (AR) was purchased from Chengdu Union Chemical Industry Reagent Re-

search Institute of China. Porous polyvinylidene fluoride (PVDF) membranes with surface pore diameter of 15 nm were purchased from Pureach Technology in China. All reagents were used as received without further purification.

2.2 Fabrication of Samples

The F2311 particles of 4 g were added to ethyl acetate of 96 g with stirring under 40 °C for 10 h to obtain the 4 wt% F2311 solution. The HMX particles were added to the F2311 solution under stirring for 10 min and then ultrasonic for 30 min, to obtain the F2311 solution with well dispersed HMX. The weight of HMX used here is 0.04 g, 0.20 g, 0.32 g, and 0.40 g, respectively. To fabricate the thin film samples, the solution was cast on the porous PVDF membrane that acts as the substrate to provide mechanical support, and dried at 30 °C in the oven. The volume fractions of HMX in the resulted films calculated by the density are 1 vol%, 5 vol %, 8 vol%, and 10 vol%, respectively. It should be mentioned that neither PBX samples nor composite films with HMX fraction higher than 10 vol% was used in this work to avoid macro-size defects in samples that complicate the data analysis.

2.3 Gas Permeation Test

The gas permeability of the films was tested at 22 °C by a constant-pressure variable-volume device with testing area of 19.26 cm^2 described in the literature [27]. N_2 pure gas was used as the feed gas, and He pure gas at 0.1 MPa was used as the sweep gas at the permeation side that carries permeated N_2 to a soap film flowmeter meter and a gas chromatography (GC, Agilent 7890B) equipped with thermal conductivity detector (TCD) that measures the concentration of N_2 at the permeation side. The gas permeability was calculated by the following equation:

$$\mathrm{P} = \frac{V \cdot l}{A \cdot t \cdot \Delta p} \tag{1}$$

where P is permeability, Barrer (1 Barrer $= 10^{-10}$ cm^3 (STP) cm cm^{-2} s^{-1} $cmHg^{-1}$); V is the volume of permeated N_2, cm^3(STP); l is the thickness of the film, cm; A is the testing area of the film, cm^2; t is the testing time, s; and Δp is the pressure difference between the feed and permeation side, cmHg. The results were reported as the mean value ± standard deviation of three samples prepared under the same condition.

2.4 Other Characterization Techniques

The morphologies of films were observed by using a scanning electronic microscope (SEM, CamScan, Apollo 300). Cross-sections of films were prepared by fracturing after immersing in liquid N_2. All samples were coated with gold by a sputter coating machine. The chemistry of films were characterized by attenuated total reflectance infrared (ATR-FTIR) spectroscopy (Nicolet 6700, Thermo Scientific of USA).

3 Gas Transport Models

The Hashemifard-Ismail-Matsuura (HIM) model was used in this work to descript the pathways of gas molecules in the films [19]. Compared with other gas transport models, the HIM model has better ability to predict permeability for films at high filler loading, which is more applicable for PBXs. In the original HIM model, the permeability of filler is also considered, while the filler in this work, i.e. explosive crystals, is impermeable to gas. Thus, the HIM model is simplified and expressed as:

$$P_r = \begin{bmatrix} 1 + \phi_{II}\left(\frac{1}{\phi_{III}\left(\lambda_i^u - 1\right)+1} - 1\right) \\ +\phi_I\left(\frac{1}{-\phi_{dI}+\phi_{II}\left(\lambda_i^u - 1\right)+1} - 1\right) \end{bmatrix}^{-u} \tag{2}$$

$$\phi_{\mathrm{I}} = \frac{\phi_d}{\pi \phi'^2_d} \tag{3}$$

$$\phi_{\mathrm{II}} = 2^{2/3} 3^{1/3} \phi'_d \theta \tag{4}$$

$$\phi_{d\mathrm{I}} = \pi \phi'^2_d \tag{5}$$

$$\phi_{i\mathrm{I}} = 4\sqrt[3]{\left(\frac{3}{2}\right)^2} \pi \phi'^2_d \left(\theta^2 + \sqrt[3]{\frac{3}{2}}\theta\right) \tag{6}$$

$$\phi_{i\mathrm{II}} = \sqrt[3]{\left(\frac{3}{2}\right)^2} \pi \phi'^2_d \left[\sqrt[3]{\left(\frac{3}{2}\right)^2} + 4\theta^2 + 4\sqrt[3]{\frac{3}{2}}\theta\right] \tag{7}$$

$$\phi'_d = \sqrt[3]{\frac{\phi_d}{\pi}} \tag{8}$$

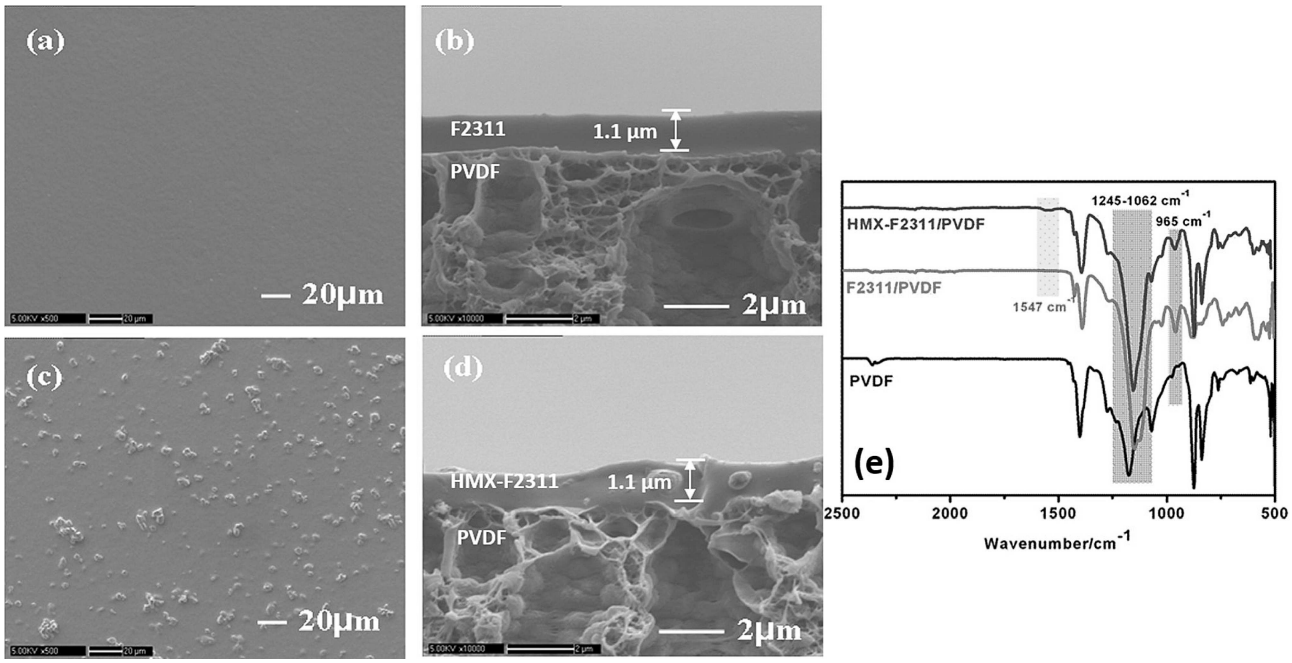

Figure 2. Characterization of samples: Morphology observed by SEM of (a) surface and (b) cross section of the F2311 film, and (c) surface and (d) cross section of the HMX-F2311 film with 10 vol% HMX, and (e) the ATR-FTIR spectra of PVDF, F2311, and HMX-F2311 films.

$$\theta = \frac{t}{d_p} \tag{9}$$

$$d_I = \sqrt[3]{\frac{3}{2}} d_p \tag{10}$$

where P_r is the gas permeability ratio of the composite film to the pure binder film; u is the exponent parameter that equals 1 for interfacial voids, but -1 for the rigidified layer; ϕ_d is the volume fraction of the dispersed explosives in the composite film; d_p is the diameter of explosive particles, mm; t is the thickness of interface, nm; λ_i is the gas permeability ratio of the interface layer to the bulk binder phase. The other parameters, such as ϕ_I and ϕ_{II}, can be calculated by the parameters given before, and the meaning of these parameters can be found in the literature [19].

For the interface with voids, the gas permeability in voids can be described by Knudsen diffusion equation as follows [28]:

$$P_i = t\sqrt{\frac{2}{RT\pi M_W}} \tag{11}$$

where P_i is the gas permeability of the interface with voids, Barrer; R is the gas constant, 8.314 $JK^{-1}mol^{-1}$; T is the testing temperature, K; M_W is the molecule weight of the gas, g mol^{-1}.

The model fitting was done by setting t as the fitting parameter in the Origin software.

4 Results and Discussion

The morphology of the F2311/PVDF film and the HMX-F2311/PVDF film with 10 vol% HMX was observed by an SEM and displayed in Figure 2 (a–d). As shown in Figure 2 (a–d), both F2311 and HMX-F2311 films on the porous PVDF substrate, are defect-free, and have the same thickness of 1.1 μm. Figure 2 (c) shows that HMX particles were well dispersed in the HMX-F2311 film. The ATR-FTIR spectra shown in Figure 2 (e) further confirm the presence of F2311 and HMX in the films. Compared with the spectrum of PVDF, there are two additional peaks in the spectrum of F2311/PVDF at 965 cm^{-1} and around 1245–1062 cm^{-1}, which are attributed to the stretching vibration of C–C and the stretching vibration of CF_2 and CF_3 of F2311, respectively [29]. Moreover, the peak present at 1547 cm^{-1} in the spectrum of HMX-F2311/PVDF, whilst not present in other spectra, is attributed to asymmetric stretching vibration of NO_2 of HMX [29]. Thus, the defect-free F2311 and HMX-F2311 films with thickness of 1.1 μm formed on the porous PVDF substrate, which is suitable for gas permeation test.

The effects of feed gas pressure and volume fraction of HMX in films on gas permeability were investigated, and the results are displayed in Figure 3. As shown in Figure 3 (a), the HMX-F2311 film possesses higher gas permeability

than the F2311 film. As the HMX crystals are impermeable to gas molecules, the increase in gas permeability after adding HMX in the film indicates that interface voids are present between HMX and F2311, which accelerate the permeation of N_2 in the HMX-F2311. The presence of these interfacial voids is further demonstrated by the variation of gas permeability with increasing feed pressure. As displayed in Figure 3 (a), the gas permeability of F2311 film is independent with the feed pressure, which indicates that the N_2 molecules transport through the F2311 film obeying solution-diffusion model as expected [30]. However, the gas permeability of HMX-F2311 film increases with increasing feed pressure, which shows that the N_2 molecules transport through interfacial voids, obeying Knudsen diffusion [28]. In order to calculate the thickness of interface layer between HMX and F2311 by using HIM model and Knudsen diffusion equation shown in Eq. (2) to (11), the gas permeability of F2311 and HMX-F2311 with HMX

volume fraction from 1 to 10 vol% was tested at a feed pressure of 0.4 MPa, and the results are displayed in Figure 3 (b). The feed pressure of 0.4 MPa was chosen due to the obvious difference in gas permeability at 0.4 MPa between HMX-F2311 to F2311 that gives more reliable value of P_r for the HIM model than that obtained at 0.2 MPa, and the lower risk of changing the structures of films than that tested at higher pressure than 0.4 MPa. With increasing volume fraction of HMX in the film, the gas permeability increases due to the increase in amount of interfacial voids. A higher volume fraction of HMX than 10 vol% was not tested, because an obvious error bar was observed for the gas permeability of HMX-F2311 with 10 vol% HMX indicating the slightly inhomogeneous distribution of HMX in F2311.

The gas permeability of F2311 and HMX-F2311 was fitted by using HIM model and Knudsen diffusion equation shown in Eq. (2) to (11), the result is shown in Figure 4. The adjusted coefficient of determination is 0.9998, indicating the high quality of the fitting result. This good fitting result confirms that the selected gas transport model is reasonable. The fitted t is 2.2 nm, which represents the thickness of the interfacial layer, with voids, between F2311 and HMX-F2311. This obtained thickness is comparable to the mean free path of the N_2 molecules, which is reasonable for Knudsen diffusion, assuming as the gas transport mechanism in the interfacial layer [28].

Considering that an interface layer with thickness about 6 nm between HMX and Estane 5703 has previously been observed by NR [18], the 2.2 nm thickness of the interface layer between HMX and F2311 elucidated here by gas permeation measurements, is comparable. According to the results of NR [18], the value of scattering length density (SLD), i.e. a function of chemistry and density of the material, at the interface is higher than that of HMX, but lower than Estane 5703. This result was attributed to the intermixing of HMX and Estane 5703 by the dissolution of HMX in the solution of Estane during sample preparation [18]. However, the results of NR could not exclude the presence of voids possessing SLD of 0 between HMX and Estane 5703. In other words, the presence of interfacial voids that may be present between HMX and Estane 5703 was ignored in the anal-

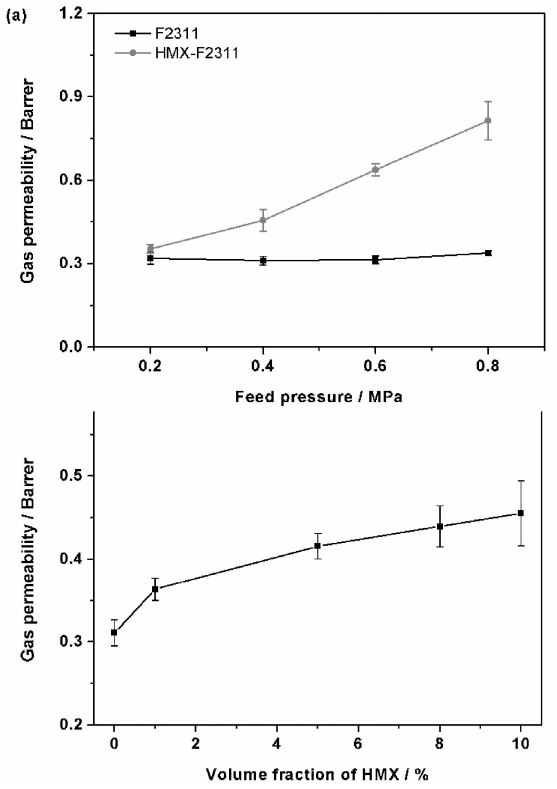

Figure 3. Gas permeability results: (a) Effects of feed gas pressure, the HMX-F2311 film contains 10 vol% HMX, and (b) Effects of volume fraction of HMX tested at feed gas pressure of 0.4 MPa.

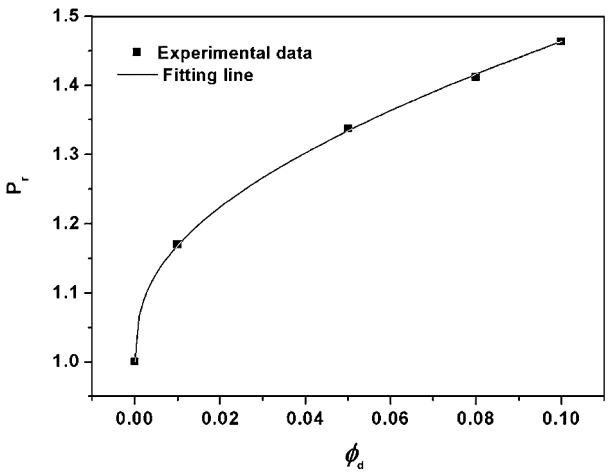

Figure 4. The Experimental and fitting gas permeability of F2311 and HMX-F2311. The model fitting was done by using HIM Model with Knudsen diffusion equation, which gives the t value of 2.2 nm with the adjusted coefficient of determination, Adj. R^2, of 0.9998.

ysis of NR results. In this work, interfacial voids were found between HMX and F2311 by gas permeation results. Moreover, these interfacial voids have also been mentioned in a prior study of thermal conductivity coefficient of PBXs [31]. The thickness of void containing interface implies that the loose contact of HMX and F2311 may be related to the surface roughness of HMX crystals. According to the previous study [26], the (011) face of HMX grows layer-by-layer through monomolecular stacking with stacking height of 0.6 nm. The thickness of interface layer between HMX and F2311 equals about four times of stacking height of (011) face of HMX, which implies the relationship between the interfacial voids and the surface roughness of HMX. Based on the results and discussion above, a schematic diagram of interface between HMX and F2311 is displayed in Figure 5. Besides HMX and F2311, voids are also present at the interface, due to the loose contact of HMX and F2311. The formation of these voids can be attributed to the poor adhesion of F2311 with HMX. It should be mentioned that the HMX-F2311 composite samples for the gas permeation test were produced at ambient temperature and ambient pressure, which is completely different from the production process of PBXs at high temperature and high pressure. In the industrial production process of PBXs, high temperature and high pressure may force the F2311 to penetrate into these interfacial voids, and form interlocking structures which enhance the adhesion between the two components. Thus, the variation of the size of interfacial voids with temperature and pressure is highly interesting and will be investigated in the future work.

5 Conclusion

A concept of characterizing interfacial micro-structures between explosive and polymer binder components, by gas permeation, has been proposed and demonstrated. Reliable N_2 permeability data were obtained by testing HMX-F2311 composite films with thickness of 1.1 μm at 0.4 MPa. The HIM model and Knudsen diffusion equation are reasonable to fit the N_2 permeability data, which gives a high adjusted coefficient of determination of 0.9998. The fitting results indicate that an interfacial layer with a thickness of 2.2 nm contains voids, which is consistent with the results of NR and thermal conductivity in the literature. The interfacial voids were considered to be related with the surface roughness of HMX crystals. This work provides an alternative characterization technique for the interfacial micro-structures between explosive and polymer binder, and gives a new insight into the interface of HMX and F2311.

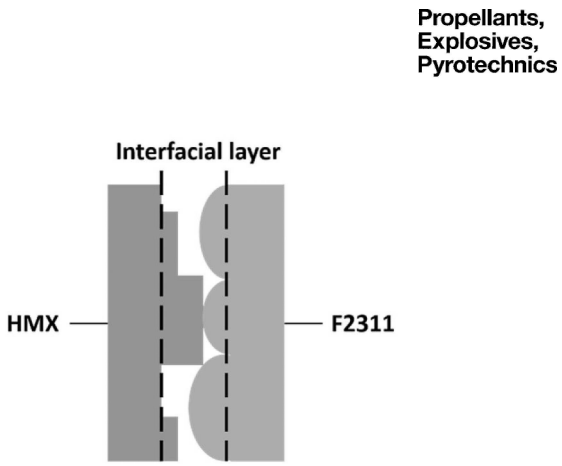

Figure 5. Schematic diagram of interface layer between HMX and F2311.

Acknowledgements

This research is supported by Science Challenge Project (TZ2018004), the Natural Science Foundation of China (No. 11572295, 21805259), the Presidential Foundation of CAEP (Grant No. 201501018), and China Scholarship Council (CSC).

References

[1] P. J. Rae, H. T. Goldrein, S. J. P. Palmer, J. E. Field, A. L. Lewis, Quasi-static studies of the deformation and failure of β-HMX based polymer bonded explosives. *Proc. R. Soc. London Ser. A* **2002**, *458*, 743–762.

[2] J. D. Yeager, E. B. Watkins, A. L. Higginbotham Duque, J. Majewski, The Thermal and Microstructural Effect of Plasticizing HMX-Nitrocellulose Composites. *J. Energ. Mater.* **2018**, *36*, 13–28.

[3] G. He, Z. Yang, L. Pan, J. Zhang, S. Liu, Q.-L. Yan, Bioinspired interfacial reinforcement of polymer-based energetic composites with a high loading of solid explosive crystals., *Journal of Materials Chemistry A.* **2017**, *5*, 13499–13510.

[4] J. D. Yeager, K. J. Ramos, R. A. Pesce-Rodriguez, S. M. Piraino, Microstructural effects of processing in the plastic-bonded explosive Composition A-3., *Mater. Chem. Phys.* **2013**, *139*, 305–313.

[5] S. J. P. Palmer, E. Field John, J. M. Huntley, Deformation, strengths and strains to failure of polymer bonded explosives. *Proc. R. Soc. London Ser. A.* **1993**, *440,* 399–419.

[6] J. D. Yeager, M. Dubey, M. J. Wolverton, M. S. Jablin, J. Majewski, D. F. Bahr, D. E. Hooks, Examining chemical structure at the interface between a polymer binder and a pharmaceutical crystal with neutron reflectometry, *Polymer.* **2011**, *52*, 3762–3768.

[7] Z. Jiang, G. Pei, X.-J. Jun, Z. Feng, X.-H. Ming, CL-20/DNB co-crystal based PBX with PEG: molecular dynamics simulation., *Modell. Simul. Mater. Sci. Eng.* **2016**, *24*, 085008.

[8] R. H. Gee, A. Maiti, S. Bastea, L. E. Fried, Molecular Dynamics Investigation of Adhesion between TATB Surfaces and Amorphous Fluoropolymers., *Macromolecules.* **2007**, *40*, 3422–3428.

[9] H. K. Springer, E. A. Glascoe, J. E. Reaugh, J. Kercher, J. L. Maienschein, Mesoscale modeling of deflagration-induced deconsolidation in polymer-bonded explosives, *AIP Conf. Proc.* **2012**, *1426*, 705–708.

[10] J. G. Bennett, K. S. Haberman, J. N. Johnson, B. W. Asay, A constitutive model for the non-shock ignition and mechanical response of high explosives., *J. Mech. Phys. Solids.* **1998**, *46*, 2303–2322.
[11] J. D. Yeager, A. M. Dattelbaum, E. B. Orler, D. F. Bahr, D. M. Dattelbaum, Adhesive properties of some fluoropolymer binders with the insensitive explosive 1,3,5-triamino-2,4,6-trinitrobenzene (TATB)., *J. Colloid Interface Sci.* **2010**, *352*, 535–541.
[12] F. Nie, J. Sun, L. Zhang, Study of Soaking Effect of Fluoropolymer Solution to TATB., *Chin. J. Energet. Mater.* **2002**, *8*, 83–85.
[13] D. J. Hoss, R. Knepper, P. J. Hotchkiss, A. S. Tappan, B. W. Boudouris, S. P. Beaudoin, An evaluation of complementary approaches to elucidate fundamental interfacial phenomena driving adhesion of energetic materials., *J. Colloid Interface Sci.* **2016**, *473*, 28–33.
[14] G. Yan, Z. Fan, S. Huang, J. Liu, Y. Wang, Q. Tian, L. Bai, J. Gong, G. Sun, X. Wang, Phase retransformation and void evolution of previously heated hmx-based plastic-bonded explosive in wet air, *J. Phys. Chem. C.* **2017**, *21*, 20426–20432.
[15] V. W. Manner, J. D. Yeager, B. M. Patterson, D. J. Walters, J. A. Stull, N. L. Cordes, D. J. Luscher, K. C. Henderson, A. M. Schmalzer, B. C. Tappan, In situ imaging during compression of plastic bonded explosives for damage modeling. *Materials.* **2017**, *10*, 638.
[16] M. Bagge-Hansen, L. Lauderbach, R. Hodgin, S. Bastea, L. Fried, A. Jones, T. Buuren, D. Hansen, J. Benterou, C. May, T. Graber, B. J. Jensen, J. Ilavsky, T. M. Willey, Measurement of carbon condensates using small-angle x-ray scattering during detonation of the high explosive hexanitrostilbene., *J. Appl. Phys.* **2015**, *117*, 245902.
[17] R.-C. Yang, Y. Tian, W.-B. Zhang, Y. Du, Study on positron lifetime of nano-void of TATB-based PBX., *Chinese Journal of Energetic Materials.* **2011**, *19*, 200–203.
[18] J. D. Yeager, K. J. Ramos, S. Singh, M. E. Rutherford, J. Majewski, D. E. Hooks, Nanoindentation of explosive polymer composites to simulate deformation and failure., *Mater. Sci. Technol.* **2012**, *28*, 1147–1155.
[19] H. Vinh-Thang, S. Kaliaguine, Predictive models for mixed-matrix membrane performance: A review, *Chem. Rev.* **2013**, *113*, 4980–5028.
[20] H. B. Park, J. Kamcev, L. M. Robeson, M. Elimelech, B. D. Freeman, Maximizing the right stuff: The trade-off between membrane permeability and selectivity, *Science*, **2017**,*356*.
[21] W. J. Koros, C. Zhang, Materials for next-generation molecularly selective synthetic membranes, *Nat. Mater.* **2017**, *16*, 289–297.
[22] G. P. Liu, V. Chernikova, Y. Liu, K. Zhang, Y. Belmabkhout, O. Shekhah, C. Zhang, S. L. Yi, M. Eddaoudi, W. J. Koros, Mixed matrix formulations with MOF molecular sieving for key energy-intensive separations., *Nat. Mater.* **2018**,*17*, 283.
[23] B. W. Asay, G. Parker, P. Dickson, B. Henson, L. Smilowitz, Dynamic measurement of the permeability of an explosive undergoing thermal damage., *J. Energ. Mater.* **2004**, *22*, 25–39.
[24] P. C. Hsu, M. DeHaven, M. McClelland, J. L. Maienschein, Thermal damage on lx-04 mock material and gas permeability assessment., *Propellants Explos. Pyrotech.* **2006**, *31*, 56–60.
[25] G. R. Parker, P. M. Dickson, B. W. Asay, L. B. Smilowitz, B. F. Henson, W. L. Perry, Understanding the mechanisms leading to gas permeation in thermally damaged pbx 9501., *AIP Conf. Proc.* **2006**, *845*, 1101–1104.
[26] Y. Jiang, J. Xu, H. Zhang, Y. Liu, L. Pu, H. Li, X. Liu, J. Sun, Growth of 2D plate-like HMX crystals on hydrophilic substrate. *Cryst. Growth Des.* **2014**, *14*, 2172–2178.
[27] S. Li, H. Zhang, S. Yu, J. Hou, S. Huang, Y. Liu, *Sep. Purif. Technol.* **2019**, *211*, 252–258.
[28] S. Matteucci, Y. Yampolskii, B. D. Freeman, I. Pinnau, *Transport of gases and vapors in glassy and rubbery polymers*, John Wiley & Sons, New York, **2006**.
[29] K. Nakanishi, P. H. Solomon, *Infrared absorption spectroscopy*, Holden-Day, San Francisco, **1977**.
[30] J. G. Wijmans, R. W. Baker RW. The solution-diffusion model: A review., *J. Membr. Sci.* **1995**, *107*
[31] X. Y. Zhao, X. M. Yang, X. W. Wei, P. Wang, The simulation of thermal conductivity coefficient of TATB-based PBX using the interface thermal resistance model. *Chin. J. Energet. Mater.* **2017**, *25*, <422–427.

Manuscript received: February 21, 2019
Revised manuscript received: April 14, 2019
Version of record online: June 6, 2019

